

LETTER • OPEN ACCESS

Evaluating the carbon capture potential of industrial waste as a feedstock for enhanced weathering

To cite this article: Pengxiao Xu and Christopher T Reinhard 2025 *Environ. Res. Lett.* **20** 044013

View the [article online](#) for updates and enhancements.

You may also like

- [The CDR potential of olivine-based enhanced rock weathering in marine systems: a case study for the coastal zone of France](#)
Luna J J Geerts, Astrid Hylén and Filip J R Meysman
- [Regional potential of coastal ocean alkalization with olivine within 100 years](#)
Murugan Ramasamy, Thorben Amann and Nils Moosdorf
- [Theoretical evaluation on CO₂ removal potential of enhanced weathering based on shrinking core model](#)
Anqi Chen, Zhuo Chen and Bo-Lin Lin

UNITED THROUGH SCIENCE & TECHNOLOGY

ECS The Electrochemical Society
Advancing solid state & electrochemical science & technology

**248th
ECS Meeting
Chicago, IL
October 12-16, 2025
Hilton Chicago**

**Science +
Technology +
YOU!**

**Register by
September 22
to save \$\$**

REGISTER NOW

This content was downloaded from IP address 72.82.254.106 on 05/08/2025 at 20:59

ENVIRONMENTAL RESEARCH LETTERS



OPEN ACCESS

RECEIVED
5 December 2024REVISED
17 February 2025ACCEPTED FOR PUBLICATION
13 March 2025PUBLISHED
21 March 2025

Original content from this work may be used under the terms of the Creative Commons Attribution 4.0 licence.

Any further distribution of this work must maintain attribution to the author(s) and the title of the work, journal citation and DOI.



LETTER

Evaluating the carbon capture potential of industrial waste as a feedstock for enhanced weathering

Pengxiao Xu* and **Christopher T Reinhard**

School of Earth and Atmospheric Sciences, Georgia Institute of Technology, Atlanta, GA 30332, United States of America

* Author to whom any correspondence should be addressed.

E-mail: pengxiao.xu@eas.gatech.edu**Keywords:** enhanced weathering, climate mitigation, carbon dioxide removal, industrial waste, Earth system modelingSupplementary material for this article is available [online](#)

Abstract

Limiting anthropogenic global climate warming since the start of the industrial period to less than 2 °C will very likely require both deep and rapid reductions in anthropogenic greenhouse gas emissions and a range of approaches toward carbon dioxide removal (CDR). One prominent CDR approach is enhanced weathering (EW), in which crushed silicate rock is applied on land or in the open ocean to accelerate natural weathering processes that absorb carbon dioxide from Earth's ocean–atmosphere system. However, in addition to a range of potential environmental, socioeconomic, and ethical issues associated with this pathway, bottlenecks in feedstock sourcing represent a key barrier for deployment of EW at scale. Here, we evaluate the potential of silicate wastes produced from industrial processes—such as steel slag and cement waste—as feedstocks for the EW process. An empirical model that links industrial alkaline waste production to gross domestic product at purchase power parity is developed to forecast waste production in the alternative futures described by the shared socioeconomic pathway (SSP) framework. By incorporating these results into an intermediate-complexity Earth system model, we also explore the impacts of EW using industrial waste on changes to global temperature, ocean pH, and ocean aragonite saturation state, while also quantifying overall CDR efficiency through the end of the century. We estimate a maximum cumulative end-of-century capture potential of ~400 GtCO₂ for industrial waste, which could represent a significant fraction of the projected CDR requirement of many mitigation scenarios in the SSP framework. However, feedstock-dependent environmental impacts and the technoconomics of feedstock redistribution may ultimately limit deployment scope.

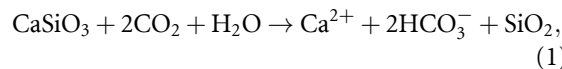
1. Introduction

Mitigating the impacts of global climate warming induced by anthropogenic emission of CO₂ and other greenhouse gases is a critical societal challenge in the coming century. In particular, there is strong impetus to limit overall climate warming since the preindustrial period to less than 2 °C, and ideally below 1.5 °C without an overshoot (Masson-Delmotte *et al* 2018, Schleussner *et al* 2024). There is increasing consensus that in order to achieve this goal conventional mitigation and decarbonization will need to be coupled with a series of carbon dioxide removal (CDR) strategies that actively remove CO₂ from the

atmosphere (Kikstra *et al* 2022, Riahi *et al* 2023). For example, even relatively optimistic emissions reduction scenarios imply ~1–10 gigatons (Gt = 10⁹ tons) of CO₂ has to be sequestered in this way every year in order to meet climate goals (e.g. Gasser *et al* 2015, Rogelj *et al* 2018a, Kikstra *et al* 2022).

One CDR method that is gaining increasing attention is enhanced weathering (EW). Broadly, this approach includes a range of practices by which alkaline (cation-rich) feedstocks are applied to croplands or surface ocean environments in order to accelerate the slow process of natural silicate weathering, which will naturally respond to excessive CO₂ emissions but only on very long timescales (Lenton

and Britton 2006, Gerdemann *et al* 2007). Using an idealized silicate mineral as a feedstock, the effective reaction can be expressed as:



or, on longer timescales:



Compared with other potential CDR approaches such as direct air capture and bioenergy with carbon capture and storage (BECCS), EW has a number of potential advantages, including relatively low energy demand, no requirement for CO₂ storage and transport infrastructure, and a range of potential agronomic and environmental co-benefits (Schuiling and Krijgsman 2006, Hartmann *et al* 2013, Taylor *et al* 2016, Beerling *et al* 2020, 2024, Li *et al* 2024). Rather than actively removing CO₂ with grid energy or using energy to capture CO₂ from biomass, CO₂ is removed passively in the form of bicarbonate or carbonate minerals as shown in reactions (1) and (2). Bicarbonate production also has the beneficial side-effect of mitigating ocean acidification because alkalinity is released during the reaction and can eventually be transferred into the ocean (Caldeira and Wickett 2005, Kanzaki *et al* 2023).

However, there are also several potential challenges and drawbacks to deploying EW at scale, including bottlenecks in the demand for feedstock to drive the process. For example, even optimistically assuming complete dissolution during deployment the maximum amount of CO₂ that can be captured per unit mass of rock is constrained by the stoichiometric ratio that governs the feedstock dissolution reaction. Equations (1) and (2) above thus imply huge amounts of rock must be extracted, processed, and transported for EW to make a tangible contribution to negative emissions in the coming decades (e.g. Hangx and Spiers 2009, Köhler *et al* 2013). For instance, olivine is regarded as a strong candidate for EW because it dissolves rapidly and has high CO₂ capture potential per unit mass (Hartmann *et al* 2013). However, current global olivine production would need to be boosted by a factor of nearly 10³ to meet the requirement of some proposed EW approaches (Kremer *et al* 2019). Even if feedstock production can be brought to this scale, extraction and processing of feedstocks implies the potential for significant additional economic and environmental costs, including lifecycle emissions of CO₂ that would reduce net negative emissions (Stler *et al* 2018, Foteinis *et al* 2023).

One possible source of alkaline feedstocks that has been previously discussed is silicate waste produced as a byproduct of industrial processes (Renforth 2019, Beerling *et al* 2020). These wastes are produced in large amounts every year and in some cases are potentially much more accessible than natural feedstocks.

For example, ~2 Gt of steel is produced every year, accompanied by approximately 0.2–0.4 Gt of steel slag, and this slag can potentially perform well as a feedstock for EW (capture potential is ~0.6 tCO₂ /t for slag, compared with 0.75 tCO₂ /t for natural wollastonite or ~0.3 tCO₂ /t for natural basalt) (Renforth 2019). Steel slag is sometimes used as an aggregate in asphalt, as raw material for cement production, or as an agricultural liming agent, but recycling rates in many countries remain low and a significant fraction of slag is instead stockpiled (Yildirim and Prezzi 2009, Gao *et al* 2023, Baalamurugan *et al* 2024), leaving large quantities available for EW. Another source for silicate waste is cement which generally has lower capture potential per unit mass but currently has the highest production among all silicate wastes (~4 Gt yr⁻¹ in 2019) (Renforth *et al* 2011, Mohamad *et al* 2022). Similar to steel slag, there are also significant stockpiles of cement waste potentially available for use in EW. By making use of cement, steel slag, and other industrial silicate wastes, it may thus be possible to reduce the need for natural feedstock extraction and circularize some fraction of industrial material fluxes. Although some CDR capacity may already be achieved through the reaction of alkaline wastes during reutilization, recycling rates of alkaline wastes are generally low, especially in developing countries that are characterized by the significant ongoing industrial production (El-Attar *et al* 2017, Gao *et al* 2023).

Recent work has attempted to estimate the carbon capture potential of silicate waste through the end of the century by using historical production data to predict future feedstock production trajectories (Renforth 2019, Beerling *et al* 2020). Here, we compile a new database for historical production of steel and cement, and provide a refined forecast for the carbon capture potential of industrial silicate wastes. An empirical model is developed that links national per capita industrial production to per-capita gross domestic product (GDP) at purchasing power parity (PPP), and uses the shared socioeconomic pathway (SSP) framework (Bauer *et al* 2017, Riahi *et al* 2017) to drive waste production forecasts until the end of the century. These are then used to evaluate the aggregate end-of-century capture potential relative to the projected negative emission requirements of different SSP mitigation scenarios. Finally, we provide the first evaluation of the potential broader impacts of EW driven by industrial waste production using an intermediate-complexity Earth system model.

2. Methods

2.1. Forecasting the CO₂ capture potential of industrial waste

We compile regional steel production data from World Steel Association, and regional cement production from USGS Mineral Industry Surveys

(figure 1), and use this database to develop an empirical model for approximate industrial waste production through 2100. The industrial wastes considered here are cement waste, steel slag, mine waste, red mud, coal ash, and biomass ash. Historical production of steel and cement are used to construct an empirical model that predicts future production and EW potential of the steel and cement industries. Carbon capture potential of other wastes, which are generally considered to have significantly lower production rates, are derived from scaling to our steel and cement forecasts according to prior estimates of normalized production of minor alkaline waste streams (Renforth 2019).

2.1.1. Historical production of steel and cement

Cement and steel are the two most common construction materials, and their production has been growing rapidly during the past several decades. For instance, according to our analysis the rate of crude steel production in 2019 was ~ 10 times that in 1950, and cement production over the same time period increased ~ 30 times. These production rates are expected to continue increasing in accordance with the growth of the global economy. In order to estimate steel and cement production to the end of this century, we use a commonly used relationship between industrial per-capita production to per-capita PPP:

$$P = a \cdot e^{\frac{-b}{\text{PPP}}}, \quad (3)$$

where P is the per capita production of steel or cement, PPP is per-capita PPP compiled from World Bank PPP and population data, and a and b are fitting constants (Renforth 2019, Beerling *et al* 2020). We opt for PPP over the nominal GDP data for two reasons: first, the SSPs database uses PPP as the primary indicator of economic growth, and we drive our future production forecasts and Earth system modeling with SSP scenarios; second, PPP-adjusted GDP is generally considered to provide a more comparable basis for assessing economic output across countries compared to nominal GDP (Gütschow *et al* 2021). We analyze six major countries and regions in the world—China, India, the United States, Russia, Brazil, and EU11, which consists of 11 countries in the European Union including the United Kingdom. We use the EU11 as a proxy for the European Union plus the UK as this grouping accounts for $\sim 80\%$ of the EU's population, GDP, and industrial production. These six countries and regions are the major contributors to global steel and cement production (figure 1).

In some cases, data from shorter historical time periods are used in order to acquire accurate fitting result from equation (3). For example, industrial development in China clearly follows different trajectories before and after the economic reformation in the 1980s and 1990s. As a result, a different

set of fitting constants is required in order to represent the high rate of industrialization in 21st century China. In the case of Russia, shifts in GDP growth and industrial development following the dissolution of the USSR require different fitting constants before and after this shift. We therefore only use data after the dissolution of the USSR and after the increase in economic and industrial development in China in order to more accurately fit equation (3) to recent developmental trajectories (figure 2). In the United States and Europe, industrial production has slowed in recent decades, with the result that the data lack a clear trend due to secular development as often characteristic of other regions. (e.g. $R^2 = 0.1$ for United States cement production). We thus use a revised fit for these regions according to:

$$P = a \cdot e^{\frac{b}{\text{PPP}^2} + \frac{c}{\text{PPP}}} \quad (4)$$

Because the United States and EU11 are on the stabilising or even declining trend of industrial production, relatively noisy fits for these two regions are unlikely to have significant impact on the accuracy of our global forecast (figure 2).

2.1.2. Forecasting carbon capture of silicate waste

2.1.2.1. Steel slag

Steel slag is a major alkaline waste product of steel production from iron ore (Shi 2004). We forecast production of steel slag through 2100 using the empirical model above and the population and economic growth projections from a given SSP assuming that approximately 117 kg of steel slag is produced for every ton of crude steel (Renforth 2019). The carbon capture potential of steel slag is calculated by summing the carbon absorbing capacity of the different alkaline components of steel slag:

$$C_p = \frac{M_{\text{CO}_2}}{100} \cdot \left(\alpha \frac{\text{CaO}}{M_{\text{CaO}}} + \beta \frac{\text{MgO}}{M_{\text{MgO}}} + \epsilon \frac{\text{Na}_2\text{O}}{M_{\text{Na}_2\text{O}}} \right. \\ \left. + \theta \frac{\text{K}_2\text{O}}{M_{\text{K}_2\text{O}}} + \gamma \frac{\text{SO}_3}{M_{\text{SO}_3}} + \delta \frac{\text{P}_2\text{O}_5}{M_{\text{P}_2\text{O}_5}} \right) \cdot 10^3 \cdot \eta, \quad (5)$$

where C_p is the overall carbon capture potential of a given mass of steel slag, CaO, MgO, Na₂O, K₂O, SO₃, P₂O₅ are elemental concentrations of Ca, Mg, Na, K, S, and P, respectively, as conventionally represented by major oxides content; and M_i is the molecular mass of oxide i (Renforth 2019). The terms α , β , ϵ , θ , γ and δ are relative contributions of each oxide to the overall slag stoichiometry, while η represents the molar quantity of CO₂ ultimately stored in the ocean for every mole of silicate reacted. Theoretically this value should be 2.0 as suggested by equation (1), but in reality the buffering of the carbonate system in terrestrial surface waters and the coastal ocean will tend to drive η to values below this. Previous studies typically employ an η value of ~ 1.5 (Renforth

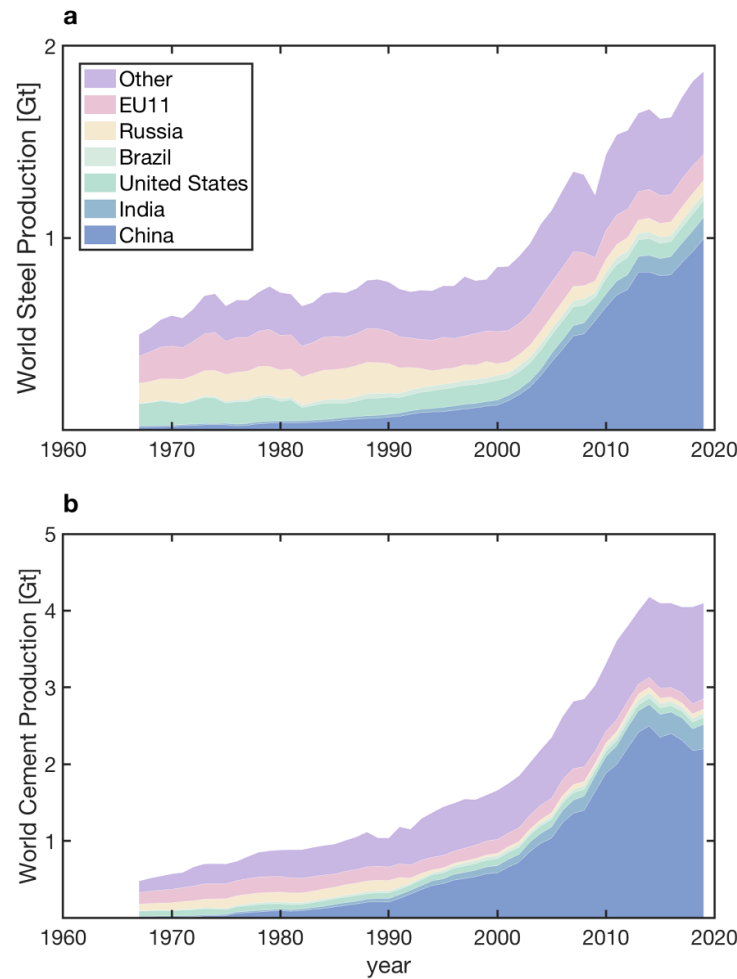


Figure 1. Historical global production of steel (a) and cement (b) in the database used here to forecast industrial waste production to the end of the century. EU11 refers to a grouping of 11 European Union nations and the United Kingdom, which we use as a proxy for industrial waste production in the European Union. ‘Other’ refers to aggregate industrial production of all other nations in the database. Data compiled from USGS (cement) and World Steel Association (steel).

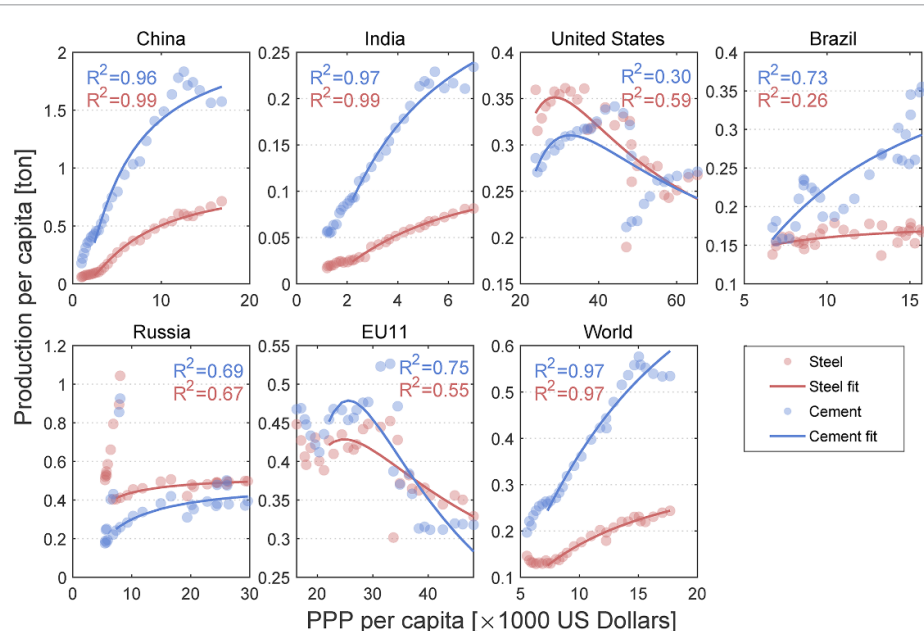


Figure 2. Historical production data of the key six countries and regions considered in our material production forecast, as well as world total production and model fitting results using equations (3) and (4).

2019, Hartmann *et al* 2013). Here, we report our results using the ideal value of $\eta = 2$, because we explicitly simulate buffering in the ocean carbonate system using an Earth system model, and thus the model directly calculates spatially varying and deployment-specific η values for different locations and emission scenarios. We consider this a more accurate approach than defining a single universal η value.

2.1.2.2. Cement waste

Cement is the most actively produced material in the construction industry, with 4 Gt of cement being produced in 2019. Production of cement through calcination of calcium carbonate at high temperature releases large quantities of CO₂ and is a significant source of emissions amongst industrial processes (Xi *et al* 2016, IEA 2022, Liu *et al* 2023). In the process of cement production, calcium oxide is produced from carbonate and used to make clinker, and this component of cement slowly absorbs CO₂ during use by diffusion of CO₂ through the cement surface. As a result, forecasting carbon capture of cement waste should include both CDR by cement during its service lifetime and the end-of-life CDR potential of cement and byproducts. We use the model of Xi *et al* (2016) to estimate CO₂ uptake during the service life of mortar and concrete cement and use this to correct the capture potential of cement waste. We also include the potential of cement kiln dust (CKD), a silicate byproduct produced in cement kilns and mostly stockpiled (El-Attar *et al* 2017), assuming that approximately 115 kg of CKD is produced for every ton of clinker. We then implement the regional average cement service lifetimes, usage patterns, and recycling ratios of Xi *et al* (2016) to estimate end-to-end capture potential of cement and cement byproducts. The carbon removal potential of cement is then calculated according to equation (4) above.

2.1.2.3. Other silicate waste

Other minor silicate wastes include mine waste, coal ash, red mud, and biomass ash. These are generally lesser material sources of EW feedstock compared with steel slag and cement waste, but also contribute to the total carbon capture of silicate waste in the aggregate (Renforth 2019, Jia *et al* 2022). Here, we assume that production rates of these wastes are related to the overall level of industrial development, and linearly scale their production to cement production rates relative to existing estimates of their individual production:

$$C_w = C_w^0 \times \frac{J_{ce}}{J_{ce}^0}, \quad (6)$$

where C_w is the aggregate carbon capture potential of mine waste, coal ash, red mud, and biomass ash used in this study, C_w^0 is a reference value for the

aggregate carbon capture potential of these wastes from Renforth (2019), and J_{ce} and J_{ce}^0 are the cement production forecasted by our model and a reference cement production flux from Renforth (2019), respectively.

2.2. Earth system modeling

2.2.1. Model description

We use the computationally efficient intermediate-complexity Earth system model cGENIE to estimate the impacts of channeling industrial waste through EW on ocean chemistry and the durability of carbon removal. We use an ocean-only configuration of cGENIE, which contains a frictional geostrophic 3D ocean circulation model (Edwards and Marsh 2005) and an energy-moisture balance model of the atmosphere coupled with a thermodynamic-dynamic sea ice model (Marsh *et al* 2011). The ocean biogeochemistry contains a nutrient-driven biological carbon pump and a full carbonate system parameterization, described in detail in Ridgwell and Hargreaves (2007), and Reinhard *et al* (2020). We use a default resolution with a 36 × 36 equal-area grid (uniform in longitude and sine of latitude) and 16 logarithmically spaced depth layers in the ocean (Marsh *et al* 2011) and seasonal forcing.

2.2.2. Model spinup and historical/future transients

The model is first spun up as a closed (ocean-atmosphere) system for 5000 years with atmospheric CO₂, CH₄, and N₂O imposed at preindustrial values to bring the ocean-atmosphere system to steady state. Historical and future transients are then branched from this spinup at model year 1765 and run until model year 2100. Atmospheric CH₄ and N₂O are concentration-driven, with abundances imposed according to a given SSP scenario, while atmospheric CO₂ is emission-driven (table 1). Historical emissions of CO₂ are first diagnosed in the model by prescribing an historical atmospheric CO₂ trajectory, with subsequent simulations using emissions trajectories diagnosed from the historical transient. Future CO₂ emission of each SSP are extracted the SSP database.

2.2.3. Carbon removal simulations

For each SSP scenario the model is run under two different conditions: (1) a control run, effectively representing an unmodified SSP scenario; and (2) an EW run, which is meant to represent the effect of channeling industrial waste through EW. In EW simulations, a certain amount of CO₂ is removed from the atmosphere, and a corresponding amount of Ca²⁺, alkalinity, and dissolved inorganic carbon are released into the ocean. Dissolved solutes from EW are introduced across the estuaries of the eight largest world rivers with fluxes proportional to their runoff (Sperna Weiland *et al* 2012), excluding the Lena and Yenisei

Table 1. Description of different SSP scenarios and forcings incorporated in the model. All forcing numbers represent values in year 2100, with CO₂ forcing defines the emission while CH₄ and N₂O forcings define the atmospheric concentrations.

SSPs	Narrative	CO ₂ forcing	CH ₄ forcing	N ₂ O forcing	References
SSP1	'Green path': the world shifts to a sustainable way of development with technology change from fossil fuels toward renewable energy. Economy growth orientated on human well-being.	24 613 Mt yr ⁻¹	1527 ppb	367 ppb	(van Vuuren <i>et al</i> 2017)
SSP2	Middle of the road: no major shift in economy, technology, and society from historic pattern. Some investment in clean energy but continue to rely on fossil fuel with medium carbon intensity.	85 684 Mt yr ⁻¹	2054 ppb	393 ppb	(Fricko <i>et al</i> 2017)
SSP3	Regional rivalry: countries focus more on domestic security and put environmental issue in low priority. Carbon intensity is high, tech development is slow due to de-globalization.	85 215 Mt yr ⁻¹	3238 ppb	421 ppb	(Fujimori <i>et al</i> 2017)
SSP4	Inequality: globally connected elites have high consumption and high-tech lifestyles while the others live a carbon intensive fuels and low-tech life. Total carbon intensity is low/medium.	44 785 Mt yr ⁻¹	2668 ppb	420 ppb	(Calvin <i>et al</i> 2017)
SSP5	Fossil-fueled development: strongly connected world with fast technology development and human capital growth, but mainly powered by non-limiting use of fossil fuels.	126 098 Mt yr ⁻¹	2598 ppb	392 ppb	(Kriegler <i>et al</i> 2017)

rivers given that they are located at latitudes that would be very unlikely to be regions of EW deployment. EW simulations are initiated in model year 2020, with changes to global average temperature, ocean pH, ocean alkalinity, and aragonite saturation state relative to the corresponding control simulation tracked from 2020 to 2100.

3. Results and discussion

3.1. Waste carbon capture potential through 2100

Our model estimates a carbon removal potential of roughly 2.7 GtCO₂ y⁻¹ in 2020 (figure 3), dominated by cement and steel production. Carbon removal potential increases gradually across all SSP scenarios, showing a mid-century flattening in carbon removal potential for all scenarios other than SSP3 which continues to increase more or less linearly through 2100. Peak carbon removal potentials range between ~5–8 GtCO₂ y⁻¹ depending on scenario, with cement and steel production representing the majority of removal potential across scenarios. Mine waste, primarily comprising materials extracted and concentrated during mining operations, is predicted to exhibit the most carbon removal potential among feedstocks other than steel slag and cement waste and even exceeds that of steel slag in certain scenarios

(figure 3). The increase in capture capacity correlates in part with the growing demand for nickel and platinum group metals in scenarios with more technology development (Renforth 2019). SSP1 is generally taken to reflect shifts toward sustainable development (van Vuuren *et al* 2017), and displays the lowest carbon removal with industrial waste. Our model is generally consistent with previous analyzes (Renforth 2019), with the exception of the SSP2 scenario which flattens at around 2060 in our analysis rather than continually increasing through the end of the century (figure 3). SSP2 is considered a 'middle-of-the-road' pathway in which society does not shift radically in terms of economy, policy, and technology from its current trajectory (Bauer *et al* 2017).

In contrast to previous analysis (Renforth 2019), we project peak carbon removal potential as being the highest for SSP3—narratively a 'regional rivalry' scenario, characterized by high challenges to mitigation and adaptation, relative provincialism in political, economic, and energy policies, relatively material-intensive consumption, and high population growth in developing countries (Fujimori *et al* 2017, Riahi *et al* 2017). The reason for this difference is not entirely clear, though our forecast is based on a somewhat crude empirical fit and subsequent analysis would benefit from a more detailed and mechanistic

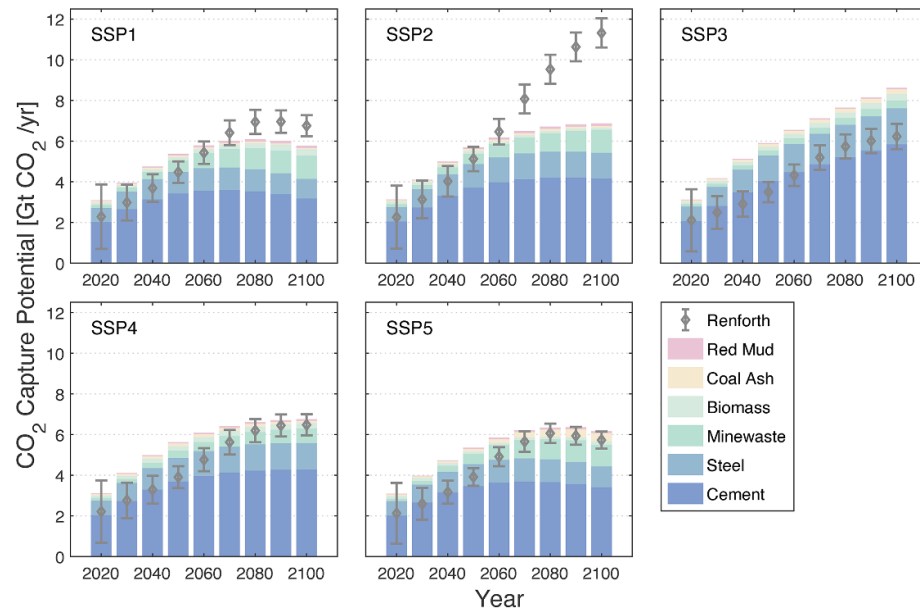


Figure 3. Projected carbon removal potential of industrial waste if channeled through enhanced weathering through the end of the century across a range of shared socioeconomic pathway (SSP) marker scenarios. Aggregate carbon removal potentials estimated by our model are broken down by waste stream, while gray dots with error bars show results from Renforth (2019).

model for regional waste production as a function of socioeconomic factors across the SSP scenario framework. This represents an important topic for future work.

The time-integrated carbon removal potential between 2020–2100 is roughly 400 GtCO₂ in total and is broadly similar across all SSP scenarios in our analysis (figure 4). This removal potential can be compared to projections of necessary negative emissions for achieving a range of SSP mitigation scenario variants, which vary considerably depending on the marker SSP and the radiative forcing target. For most scenarios, the time-integrated carbon removal potential of industrial waste is comparable to negative emissions projections for BECCS and forestry carbon removal. (figure 4). For low-emission scenarios (SSP1-3.4, SSP1-4.5), the time-integrated carbon removal potential of industrial waste could be larger than the combined impacts of BECCS, the forestry sector, and point-source carbon capture and storage. However, more emissions-intensive scenarios with lower radiative forcing targets require more total negative emissions from BECCS and forestry than our analysis suggests is possible with carbon removal using industrial waste (figure 4).

It is important to emphasize that our estimates of carbon removal potential represent maximum values, and there are several factors that might decrease removal potential in practice. First, we expect that there will often be a mismatch between the locations of alkaline waste production and regions of EW deployment (figure 5). As a result, processing and redistribution of the industrial waste will lead to life cycle carbon emissions and technoeconomic

impacts that will almost certainly reduce overall carbon removal efficiency. Although it is generally assumed that the carbon intensity of these processes is relatively small compared with overall removal potential (Renforth 2012, Strefler *et al* 2018), we would expect that the transport costs associated with waste redistribution may also significantly impact dollar-per-ton costs of CDR. In any case, these impacts would be expected to vary considerably from project to project and would need to be evaluated on a regional basis moving forward. Second, potential toxicity of heavy metals released from some waste streams might also limit the overall capacity of carbon removal. For example, some slag streams may have elevated levels of heavy metals such as Pb, Ni, Cr, and Cd, which could be released to soils and groundwaters (Hu *et al* 2020). Taking China as an example, using the agricultural land data from World Bank we estimate that if EW were to be deployed on 50% of agricultural land in China approximately 360 t km⁻² yr⁻¹ of steel slag would need to be added in order to achieve the full carbon removal potential estimated here. Although this is a relatively low feedstock application rate for an EW deployment, metal content can vary over orders of magnitude in industrial waste feedstocks and the accumulation of heavy metals Cr in soil might still significantly reduce deployment scope in some cases.

In the cement industry, combustible waste is increasingly utilized as fuel for cement production in order to reduce costs, but this practice can lead to elevated concentrations of heavy metals in cement clinker. Minimizing environmental toxicity might either reduce the total amount of feedstock that can

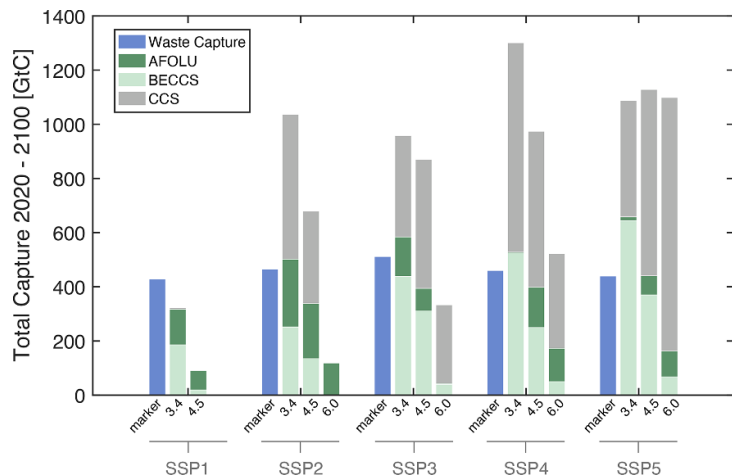


Figure 4. Time-integrated carbon removal potential of industrial waste if channeled through enhanced weathering through the end of the century across a range of shared socioeconomic pathway (SSP) scenarios. Bars show total carbon removed between 2020–2100 for each scenario, with ‘Waste Capture’ referring to carbon removal resulting from industrial waste production channeled through enhanced weathering in each SSP marker scenario. Scenario designations refer to total carbon capture for a given mitigation scenario disaggregated into bioenergy with carbon capture and storage (BECCS) and land-use practices (AFOLU), which constitute true carbon removal, together with point-source carbon capture and storage (CCS). For instance, Scenario SSP2-3.4 represents an SSP2 (‘middle of the road’) pathway with a mitigation scenario capable of capping global radiative forcing to 3.4 W m^{-2} at the end of the century. Note that there is no SSP1-6.0 in the scenario database because this scenario requires no carbon removal to achieve a radiative forcing of 6.0 W m^{-1} in 2100.

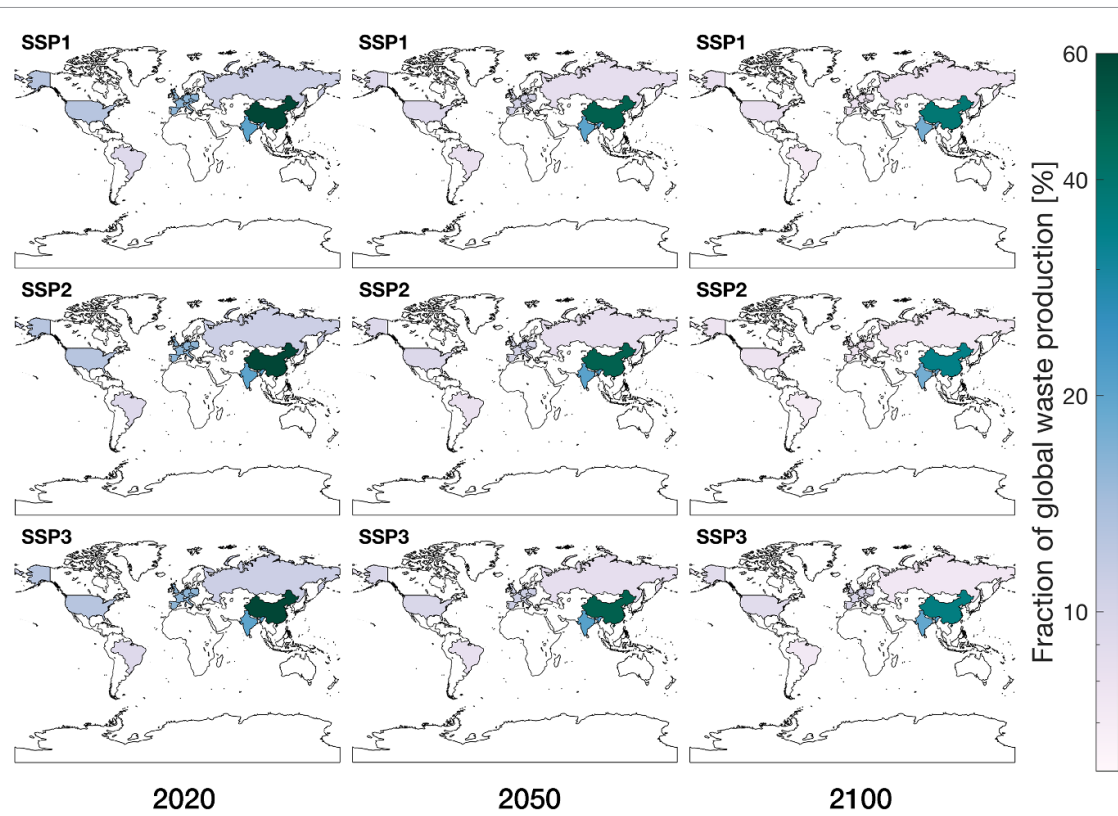


Figure 5. Spatial distribution of alkaline waste production from a subset of the shared socioeconomic pathway (SSP) scenarios explored here, for 2020, 2050, and end-of-century. Note the log scale.

be deployed per unit area or could require additional remediation steps in waste processing which could both induce additional carbon emission (Gao *et al* 2023) and impact costs. This remains a critically

important topic for future work, and we argue that any attempt to utilize industrial waste as a feedstock for EW must scrupulously foreground this issue and transparently document steps mitigation.

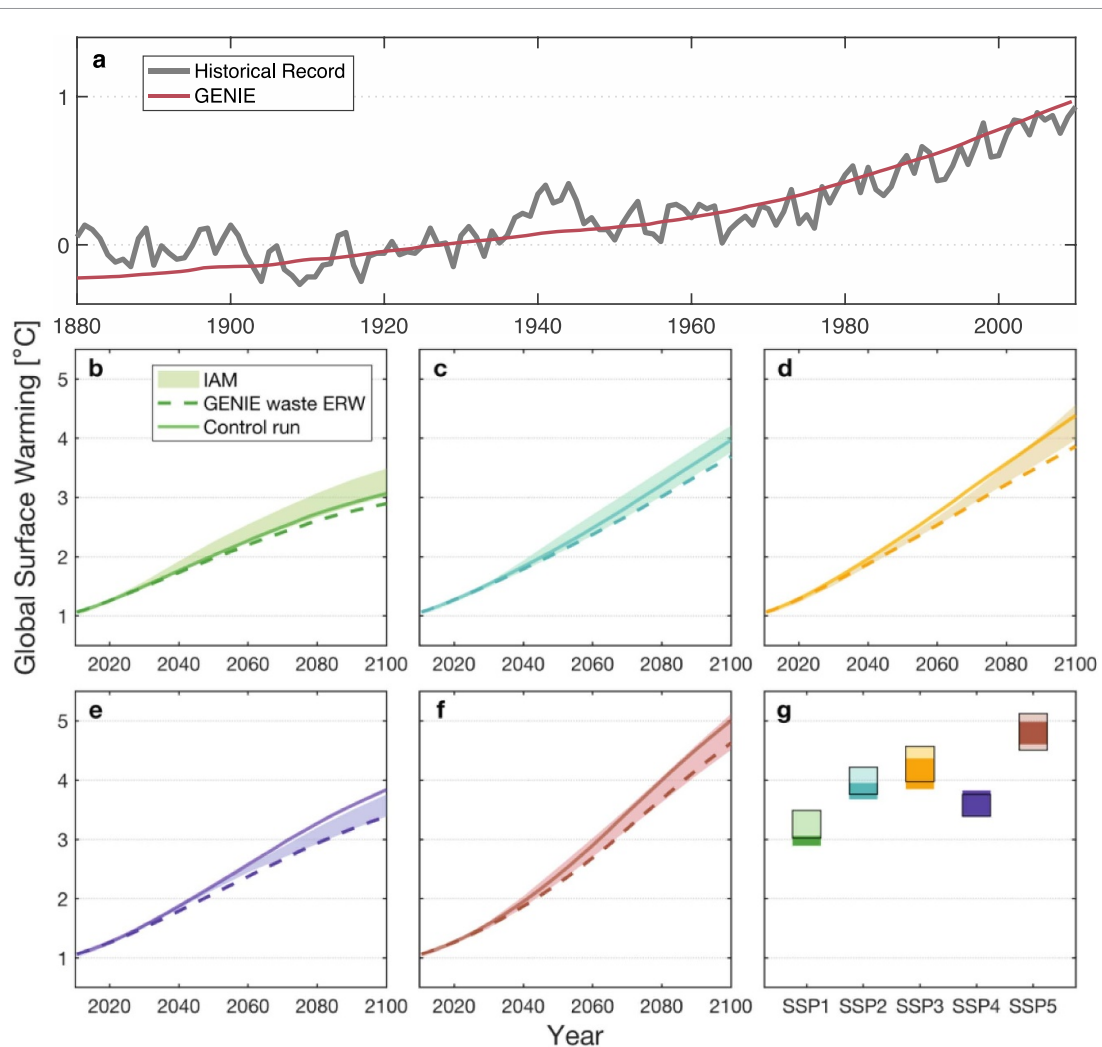


Figure 6. Impact of channeling industrial silicate wastes through enhanced weathering on global climate warming for a range of shared socioeconomic pathway (SSP) scenarios. (a) Global temperature in cGENIE simulation compared with the historical temperature record based on data from National Centers for Environmental Information; (b)–(f) temperature trajectories for scenario SSP1, SSP2, SSP3, SSP4, and SSP5, respectively; (g) overall temperature shift between control and EW simulations in 2100, together with the uncertainty range from integrated assessment models (IAMs).

3.2. Impacts on the Earth system

3.2.1. Global temperature

We evaluate global temperature shifts relative to the time-integrated average pre-industrial temperature between 1850–1900. The global temperature trajectories in our control historical transients are for the most part well within the range of previous results from integrated assessment models (IAMs) for the SSP marker scenarios (Riahi *et al* 2017, Rogelj *et al* 2018b, Gidden *et al* 2019), with the exception of SSP4 for which our simulated temperatures are slightly higher than the IAM range (figure 6). Implementation of EW using industrial wastes as a feedstock leads to systematic but relatively small decreases in global temperature relative to SSP marker scenario simulations, with an overall temperature decrease in model year 2100 ranging between ~ 0.17 °C for SSP1 to ~ 0.5 °C for SSP3 (figure 6(f)).

Taken in isolation, carbon removal through EW with industrial wastes as a feedstock has a trivial impact on global temperature in marker scenarios, with temperature differences in 2100 that are within the uncertainty of IAM trajectories. On the other hand, these relatively modest temperature shifts can become more important in scenarios that feature more rapid and aggressive emissions mitigation. For example, in our simulation of SSP2-1.9, which is designed to limit the overall warming in 2100 below the 1.5 °C threshold, the addition of EW using industrial wastes as a feedstock further reduces the average warming in 2100 to ~ 1.1 °C (figure 7(a)). Nevertheless, taken together our results further emphasize the clear need to focus foremost on mitigation of anthropogenic greenhouse gas emissions rather than deterring mitigation based on the actual or perceived potential of carbon removal pathways (Bertram *et al* 2018, Riahi *et al* 2023).

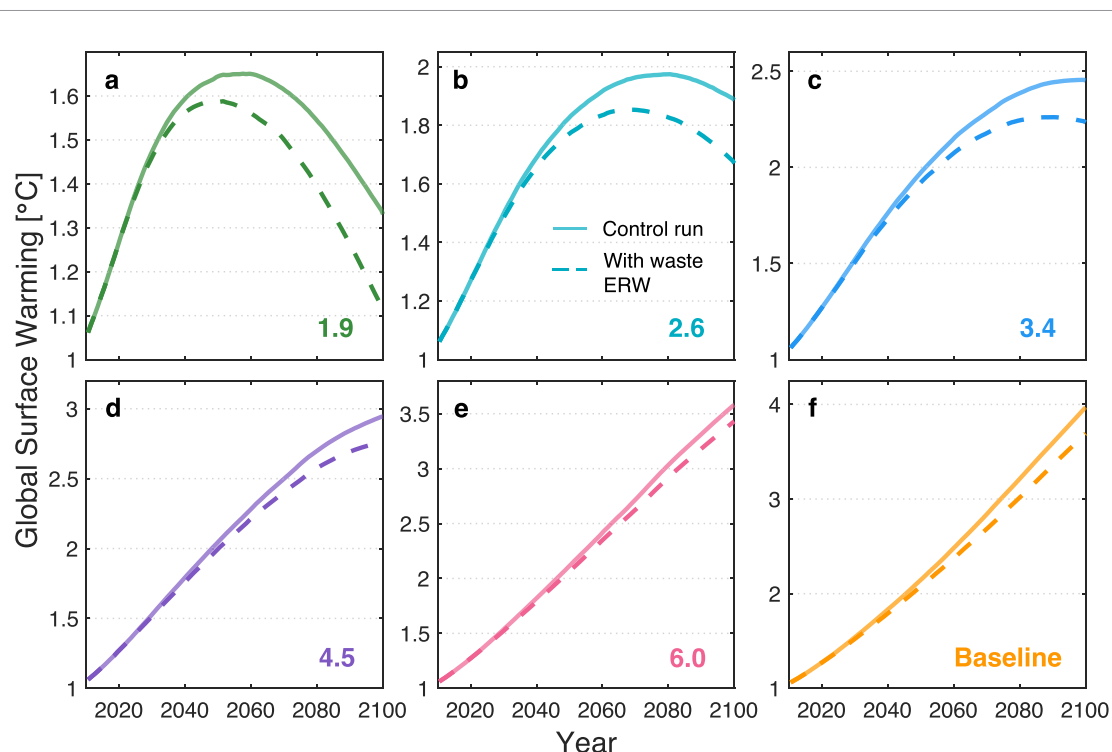


Figure 7. The impact of channeling industrial silicate wastes through enhanced weathering on global climate warming through 2100 for SSP2 baseline and mitigation scenarios.

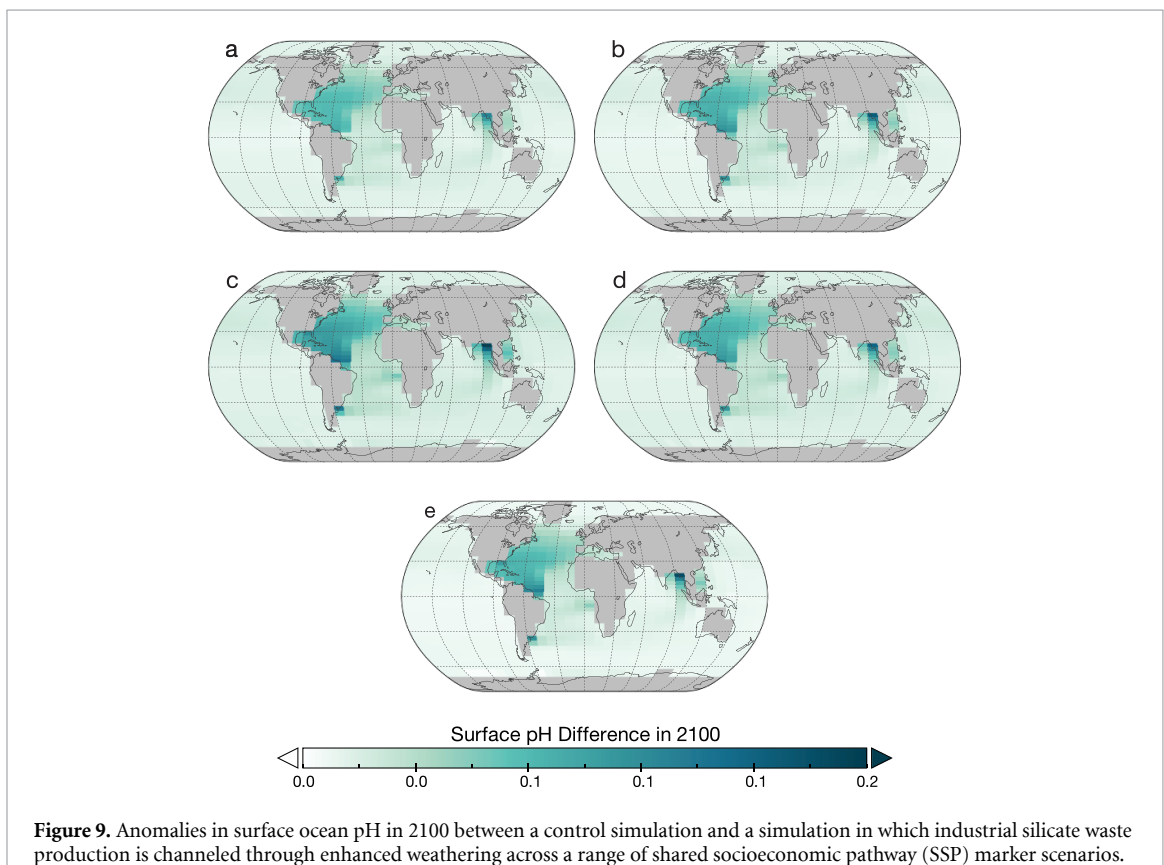
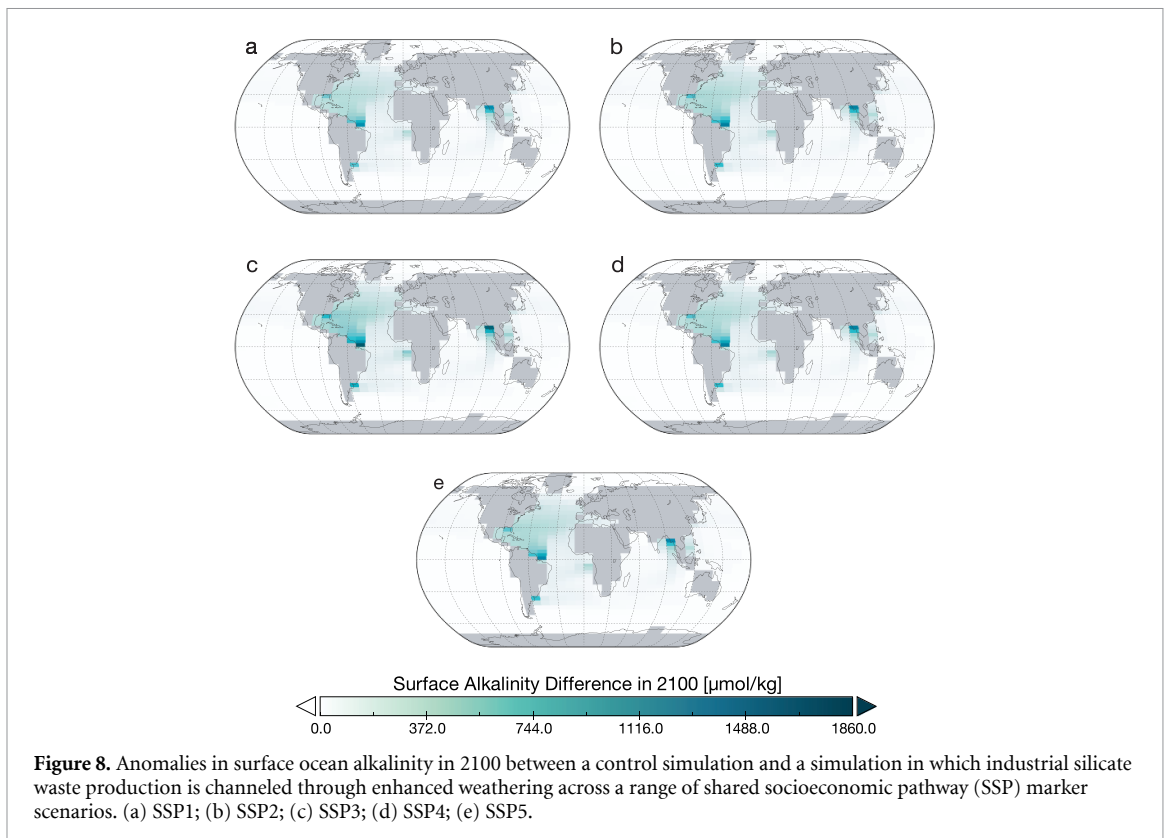
3.2.2. Ocean carbon chemistry

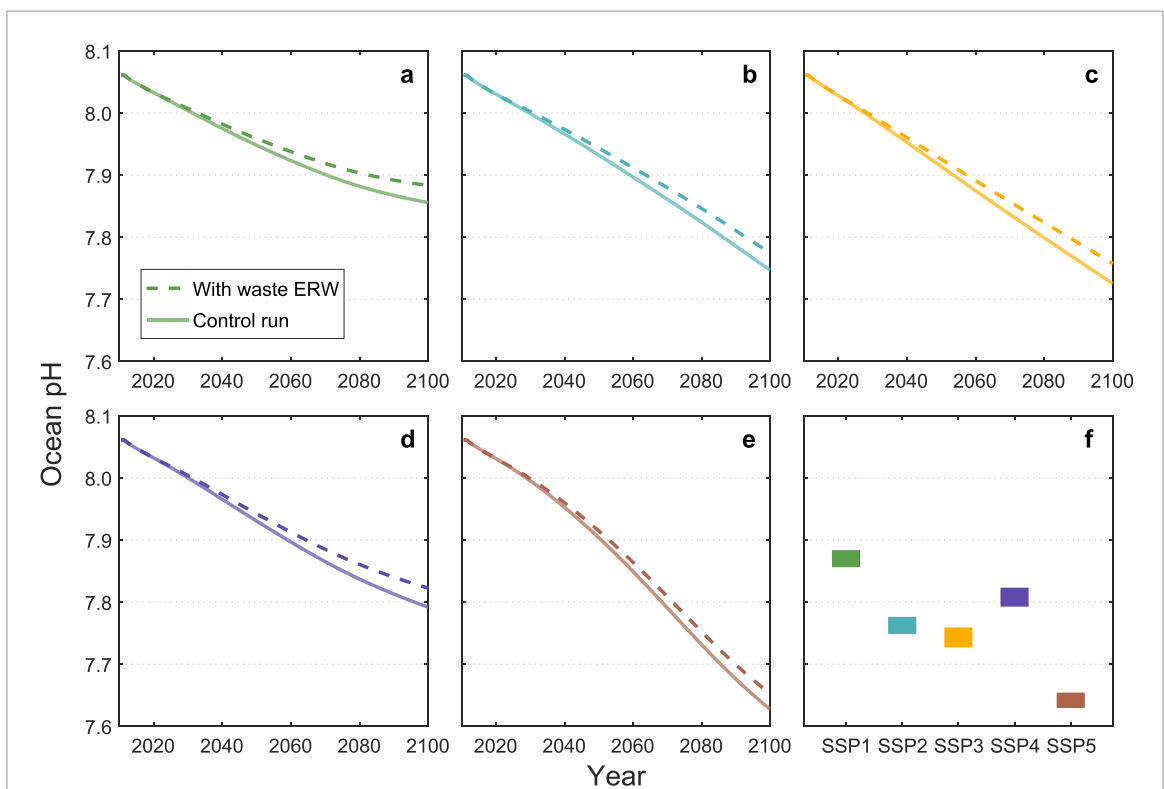
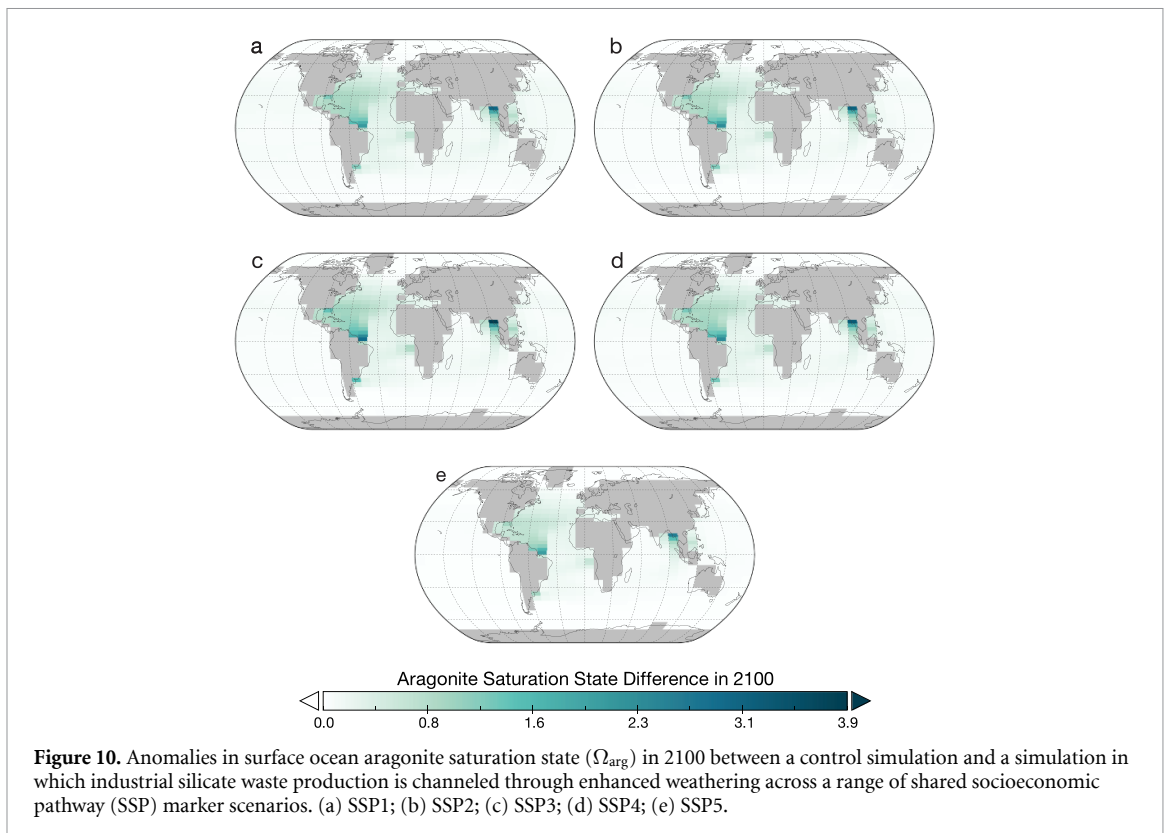
One potential co-benefit of EW is an introduction of alkalinity to coastal surface ocean waters, which could potentially help to mitigate ongoing ocean acidification induced by anthropogenic CO₂ release (Hartmann *et al* 2013, Taylor *et al* 2016, Renforth and Campbell 2021). Indeed, our simulations are characterized by clear zones of elevated alkalinity near river mouths across all SSPs (figure 8), and commensurate regional increases in ocean pH in the same locations (figure 9). These impacts lead to locally significant increases in aragonite saturation state (Ω_{arg} ; figure 10), a critical parameter regulating biogenic calcification in shallow marine habitats (e.g. Kleypas *et al* 1999). Although changes to ocean pH and Ω_{arg} in our simulations are relatively minor on the basin scale (figures 11 and 12), local/regional impacts can be significant and, in some cases, would be expected to have tangible impacts on coral calcification rates (Gattuso *et al* 1998, Albright *et al* 2008, Erez *et al* 2011). However, it is unlikely that impacts of this scale will be sufficient to counteract the damaging impacts of increased surface ocean temperatures in less mitigation-intensive scenarios (Laufkötter *et al* 2020), and significant uncertainty remains in the dynamics of coastal ocean alkalinity modification, whether through terrestrial EW approaches or through ocean-based pathways (Burt *et al* 2021, National Academies of Sciences, Engineering, and Medicine 2022). Further investigation of regional variability in ocean chemistry and synergistic effects

with temperature are important topics for future research.

4. Conclusions

Global mass fluxes of silicate industrial wastes will be significant through the end of the century across a range of SSP scenarios. If channeled through EW, this waste stream could be used to drive carbon removal at the gigaton scale. However, the impacts of this on carbon budgets and climate warming will be negligible unless coupled with rapid and aggressive mitigation of anthropogenic greenhouse gas emissions. Potential co-benefits associated with ocean alkalinity modification on the scales implied by silicate industrial waste production would be relatively small on the basin or global scale but could be locally significant. Industrial silicate wastes will vary in their composition and potential environmental impacts (Mohamad *et al* 2022), and there are currently active debates surrounding the design principles of responsible practice in EW, including the need to accurately quantify weathering rates at the field scale (Knapp *et al* 2023, Reershemius *et al* 2023) possible downstream leakage of initially captured CO₂ in river/stream systems (Zhang *et al* 2022, Harrington *et al* 2023) and the coastal ocean (Kanzaki *et al* 2023) and appropriate models for incentivization. Nevertheless, our results add to a growing body of work indicating that silicate waste streams may have potential for use in carbon





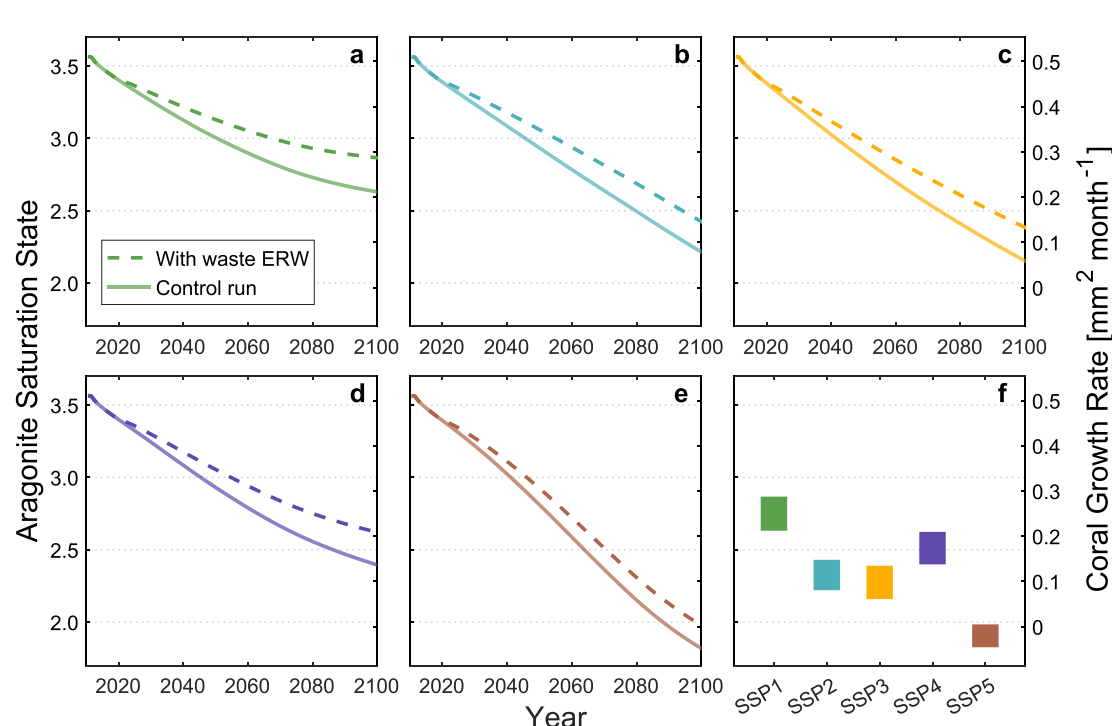


Figure 12. Impacts of channeling industrial silicate wastes through enhanced weathering on average aragonite saturation state (Ω_{arg}) between 30°N and 30°S for a range of shared socioeconomic pathway (SSP) scenarios. (a) SSP1; (b) SSP2; (c) SSP3; (d) SSP4; (e) SSP5. Panel (f) shows the global difference in Ω_{arg} between control and EW simulations in 2100. The right-hand y -axis scales Ω_{arg} to coral calcification rate according to the relationship in Albright *et al* (2008). We stress that this represents a single experimental suite with one coral species, so is only meant to be broadly illustrative of potential impacts of emissions trajectories and carbon removal mitigation on coral calcification rate.

removal deployments (Pullin *et al* 2019, Bullock *et al* 2021, Aviso *et al* 2022, Jia *et al* 2022, Power *et al* 2024).

Christopher T Reinhard <https://orcid.org/0000-0002-2632-1027>

Data availability statement

The data that support the findings of this study are openly available at the following URL/DOI: <https://zenodo.org/records/11187754>.

Acknowledgment

The authors wish to acknowledge support from the Partnership for an Advanced Computing Environment (PACE) at the Georgia Institute of Technology. CTR acknowledges funding from the U.S. Department of Energy and the Grantham Foundation.

Open Research

All observational datasets are available from the references provided. The Earth system model code will be rendered publicly available as a tagged release archived with a permanent DOI at [10.5281/zenodo.11187754](https://doi.org/10.5281/zenodo.11187754).

ORCID iDs

Pengxiao Xu <https://orcid.org/0009-0006-3372-4293>

References

- Albright R, Mason B and Langdon C 2008 Effect of aragonite saturation state on settlement and post-settlement growth of *Porites astreoides* larvae *Coral Reefs* **27** 485–90
- Aviso K B, Lee J Y, Ubando A T and Tan R R 2022 Fuzzy optimization model for enhanced weathering networks using industrial waste *Clean Technol. Environ. Policy* **24** 21–37
- Baalamurugan J, Kumar V G, Padmapriya R and Raja V K B 2024 Recent applications of steel slag in construction industry *Environ. Dev. Sustain.* **26** 2865–96
- Bauer N *et al* 2017 Shared socio-economic pathways of the energy sector—quantifying the narratives *Glob. Environ. Change* **42** 316–30
- Beerling D *et al* 2020 Potential for large-scale CO₂ removal via enhanced rock weathering with croplands *Nature* **583** 242–8
- Beerling D J *et al* 2024 Enhanced weathering in the US Corn Belt delivers carbon removal with agronomic benefits *Proc. Natl Acad. Sci. USA* **121** e2319436121
- Bertram C, Luderer G, Popp A, Minx J C, Lamb W F, Stevanović M, Humpenöder F, Giannousakis A and Kriegler E 2018 Targeted policies can compensate most of the increased sustainability risks in 1.5 °C mitigation scenarios *Environ. Res. Lett.* **13** 64038
- Bullock L A, James R H, Matter J, Renforth P and Teagle D A H 2021 Global carbon dioxide removal potential of waste materials from metal and diamond mining *Front. Clim.* **3** 694175
- Burt D J, Fröb F and Ilyina T 2021 The sensitivity of the marine carbonate system to regional ocean alkalinity enhancement *Front. Clim.* **3** 624075

- Caldeira K and Wickett M 2005 Ocean model predictions of chemistry changes from carbon dioxide emissions to the atmosphere and ocean *J. Geophys. Res. C* **110** 1–12
- Calvin K *et al* 2017 The SSP4: a world of deepening inequality *Glob. Environ. Change* **42** 284–96
- Edwards N R and Marsh R 2005 Uncertainties due to transport-parameter sensitivity in an efficient 3-D ocean-climate model *Clim. Dyn.* **24** 415–33
- El-Attar M M, Sadek D M and Salah A M 2017 Recycling of high volumes of cement kiln dust in bricks industry *J. Clean. Prod.* **143** 506–15
- Erez J, Reynaud S, Silverman J, Schneider K and Allemand D 2011 *Coral Calcification under Ocean Acidification and Global Change BT—Coral Reefs: An Ecosystem in Transition* ed Z Dubinsky and N Stambler (Springer Netherlands) pp 151–76
- Foteinis S, Campbell J S and Renforth P 2023 Life cycle assessment of coastal enhanced weathering for carbon dioxide removal from air *Environ. Sci. Technol.* **57** 6169–78
- Fricko O *et al* 2017 The marker quantification of the shared socioeconomic pathway 2: a middle-of-the-road scenario for the 21st century *Glob. Environ. Change* **42** 251–67
- Fujimori S, Hasegawa T, Masui T, Takahashi K, Herran D S, Dai H, Hijioka Y and Kainuma M 2017 SSP3: AIM implementation of shared socioeconomic pathways *Glob. Environ. Change* **42** 268–83
- Gao W, Zhou W, Lyu X, Liu X, Su H, Li C and Wang H 2023 Comprehensive utilization of steel slag: a review *Powder Technol.* **422** 118449
- Gasser T, Guivarch C, Tachiiri K, Jones C D and Ciais P 2015 Negative emissions physically needed to keep global warming below 2 °C *Nat. Commun.* **6** 7958
- Gattuso J-P, Frankignoulle M, Bourge I, Romaine S and Buddemeier R W 1998 Effect of calcium carbonate saturation of seawater on coral calcification *Glob. Planet Change* **18** 37–46
- Gerdemann S J, O'Connor W K, Dahlin D C, Penner L R and Rush H 2007 Ex situ aqueous mineral carbonation *Environ. Sci. Technol.* **41** 2587–93
- Gidden M J *et al* 2019 Global emissions pathways under different socioeconomic scenarios for use in CMIP6: a dataset of harmonized emissions trajectories through the end of the century *Geosci. Model Dev.* **12** 1443–75
- Gütschow J, Louise Jeffery M, Günther A and Meinshausen M 2021 Country-resolved combined emission and socio-economic pathways based on the representative concentration pathway (RCP) and shared socio-economic pathway (SSP) scenarios *Earth Syst. Sci. Data* **13** 1005–40
- Hangx S J T and Spiers C J 2009 Coastal spreading of olivine to control atmospheric CO₂ concentrations: a critical analysis of viability *Int. J. Greenhouse Gas Control* **3** 757–67
- Harrington K J, Hilton R G and Henderson G M 2023 Implications of the riverine response to enhanced weathering for CO₂ removal in the UK *Appl. Geochem.* **152** 105643
- Hartmann J *et al* 2013 Enhanced chemical weathering as a geoengineering strategy to reduce atmospheric carbon dioxide, supply nutrients, and mitigate ocean acidification *Rev. Geophys.* **51** 113–49
- Hu R, Xie J, Wu S, Yang C and Yang D 2020 Study of toxicity assessment of heavy metals from steel slag and its asphalt mixture *Materials* **13** 2768
- IEA 2022 CO₂ emissions in 2022
- Jia X, Zhang Z, Wang F, Li Z, Wang Y, Aviso K B, Foo D Y C, Nair P N S B, Tan R R and Wang F 2022 Regional carbon drawdown with enhanced weathering of non-hazardous industrial wastes *Resour. Conserv. Recycl.* **176** 105910
- Kanzaki Y, Planavsky N J, Reinhard C T and Abbott D 2023 New estimates of the storage permanence and ocean co-benefits of enhanced rock weathering *PNAS Nexus* **2** pgad059
- Kikstra J S *et al* 2022 The IPCC sixth assessment report WGIII climate assessment of mitigation pathways: from emissions to global temperatures *Geosci. Model Dev.* **15** 9075–109
- Kleypas J A, Buddemeier R W, Archer D, Gattuso J-P, Langdon C and Opdyke B N 1999 Geochemical consequences of increased atmospheric carbon dioxide on coral reefs *Science* **284** 118–20
- Knapp W J *et al* 2023 Quantifying CO₂ removal at enhanced weathering sites: a multiproxy approach *Environ. Sci. Technol.* **57** 9854–64
- Köhler P, Abrams J F, Völker C, Hauck J and Wolf-Gladrow D A 2013 Geoengineering impact of open ocean dissolution of olivine on atmospheric CO₂, surface ocean pH and marine biology *Environ. Res. Lett.* **8** 014009
- Kremer D, Etzold S, Boldt J, Blaum P, Hahn K M, Wotrubá H and Telle R 2019 Geological mapping and characterization of possible primary input materials for the mineral sequestration of carbon dioxide in Europe *Minerals* **9** 485
- Kriegler E *et al* 2017 Fossil-fueled development (SSP5): an energy and resource intensive scenario for the 21st century *Glob. Environ. Change* **42** 297–315
- Laufkötter C, Zscheischler J and Frölicher T L 2020 High-impact marine heatwaves attributable to human-induced global warming *Science* **369** 1621–5
- Lenton T M and Britton C 2006 Enhanced carbonate and silicate weathering accelerates recovery from fossil fuel CO₂ perturbations *Glob. Biogeochem. Cycles* **20** 3
- Li Z, Planavsky N J and Reinhard C 2024 Geospatial assessment of the cost and energy demand of feedstock grinding for enhanced rock weathering in the coterminous United States *Front. Clim.* **6** 1380651
- Liu Z, Deng Z, Davis S and Ciais P 2023 Monitoring global carbon emissions in 2022 *Nat. Rev. Earth Environ.* **4** 205–6
- Marsh R, Müller S A, Yool A and Edwards N R 2011 Incorporation of the C-GOLDSTEIN efficient climate model into the GENIE framework: “eb_go_gs” configurations of GENIE *Geosci. Model Dev.* **4** 957–92
- Masson-Delmotte V, Zhai P, Pörtner H-O, Roberts D, Skea J and Shukla P R 2018 Global warming of 1.5 °C *IPCC—Sr15* 2 17–20 (available at: www.environmentalgraphiti.org/)
- Mohamad N, Muthusamy K, Embong R, Kusbiantoro A and Hashim M H 2022 Environmental impact of cement production and solutions: a review *Mater. Today: Proc.* **48** 741–6
- National Academies of Sciences, Engineering, and Medicine 2022 A research strategy for ocean-based carbon dioxide removal and sequestration (<https://doi.org/10.17226/26278>)
- Power I M, Paulo C and Rausis K 2024 The mining industry’s role in enhanced weathering and mineralization for CO₂ removal *Environ. Sci. Technol.* **58** 43–53
- Pullin H, Bray A W, Burke I T, Muir D D, Sapsford D J, Mayes W M and Renforth P 2019 Atmospheric carbon capture performance of legacy iron and steel waste *Environ. Sci. Technol.* **53** 9502–11
- Reershemius T *et al* 2023 Initial validation of a soil-based mass-balance approach for empirical monitoring of enhanced rock weathering rates *Environ. Sci. Technol.* **57** 19497–507
- Reinhard C T, Olson S L, Kirtland Turner S, Pälike C, Kanzaki Y and Ridgwell A 2020 Oceanic and atmospheric methane cycling in the cGENIE Earth system model—release v0.9.14 *Geosci. Model Dev.* **13** 5687–706
- Renforth P 2012 The potential of enhanced weathering in the UK *Int. J. Greenh. Gas Control* **10** 229–43
- Renforth P 2019 The negative emission potential of alkaline materials *Nat. Commun.* **10** 1401
- Renforth P and Campbell J S 2021 The role of soils in the regulation of ocean acidification *Phil. Trans. R. Soc. B* **376** 20200174

- Renforth P, Washbourne C L, Taylder J and Manning D A C 2011 Silicate production and availability for mineral carbonation *Environ. Sci. Technol.* **45** 2035–41
- Riahi K *et al* 2017 The shared socioeconomic pathways and their energy, land use, and greenhouse gas emissions implications: an overview *Glob. Environ. Change* **42** 153–68
- Riahi K *et al* 2023 Mitigation pathways compatible with long-term goals *Climate Change 2022—Mitigation of Climate Change* (Cambridge University Press) pp 295–408
- Ridgwell A and Hargreaves J C 2007 Regulation of atmospheric CO₂ by deep-sea sediments in an Earth system model *Glob. Biogeochem. Cycles* **21** 2
- Rogelj J *et al* 2018a Mitigation pathways compatible with 1.5 °C in the context of sustainable development *IPCC Special Report Global Warming of 1.5 °C* p 82
- Rogelj J *et al* 2018b Scenarios towards limiting global mean temperature increase below 1.5 °C *Nat. Clim. Change* **8** 325–32
- Schleussner C-F *et al* 2024 Overconfidence in climate overshoot *Nature* **634** 366–73
- Schuiling R D and Krijgsman P 2006 Enhanced weathering: an effective and cheap tool to sequester CO₂ *Clim. Change* **74** 349–54
- Shi C 2004 Steel slag—its production, processing, characteristics, and cementitious properties *J. Mater. Civil Eng.* **16** 230–6
- Sperna Weiland F C, Van Beek L P H, Kwadijk J C J and Bierkens M F P 2012 Global patterns of change in discharge regimes for 2100 *Hydrol. Earth Syst. Sci.* **16** 1047–62
- Strefler J, Amann N, Bauer N, Kriegler E and Hartmann J 2018 Potential and costs of carbon dioxide removal by enhanced weathering of rocks *Environ. Res. Lett.* **13** 034010
- Taylor L L, Quirk J, Thorley R M S, Kharecha P A, Hansen J, Ridgwell A, Lomas M R, Banwart S A and Beerling D J 2016 Enhanced weathering strategies for stabilizing climate and averting ocean acidification *Nat. Clim. Change* **6** 402–6
- van Vuuren D P *et al* 2017 Energy, land-use and greenhouse gas emissions trajectories under a green growth paradigm *Glob. Environ. Change* **42** 237–50
- Xi F *et al* 2016 Substantial global carbon uptake by cement carbonation *Nat. Geosci.* **9** 880–3
- Yildirim I and Prezzi M 2009 *Use of Steel Slag in Subgrade Applications* FHWA/IN/JTRP-2009/32 (Joint Transportation Research Program, Indiana Department of Transportation and Purdue University) (<https://doi.org/10.5703/1288284314275>)
- Zhang S, Planavsky N J, Katchinoff J, Raymond P A, Kanzaki Y, Reershemius T and Reinhard C T 2022 River chemistry constraints on the carbon capture potential of surficial enhanced rock weathering *Limnol. Oceanogr.* **67** S148–57